Chapter 7

Feldspar and Clay Mineralogy

Theresa E. McReynolds, Sheldon A. Skaggs, and Paul A. Schroeder

To refine our understanding of the differences between clay-resource regions, 42 clay samples were analyzed by X-ray diffraction (XRD; Table B.6; Figure 7.1). The primary purpose of the analyses was to identify variability in mineral assemblages that could explain the geochemical patterns described in Chapter 5. An additional objective was to evaluate the relationship between mineralogy and the performance characteristics evaluated in Chapter 4.

X-Ray Diffraction

Plastic soils are typically mixtures of one or more clay minerals and nonclay minerals such as feldspar, quartz, and micas (Klein and Hurlbut 1993:512). Most of the nonclay components are identifiable in thin section, but clay minerals are so small (< 2 μm in spherical diameter) that they can only be recognized on the basis of their crystalline structures. Four groups of clay minerals are distinguished according to their three-dimensional arrangements of atoms: (1) the kaolin group (including kaolinite, halloysite, nacrite, and dickite); (2) the smectite group (including montmorillonite, nontronite, saponite, sauconite, and vermiculite); (3) illite; and (4) chlorite (including clinoclore and chamosite). Any two of these clay mineral groups can also occur together in mixed layers.

XRD is uniquely capable of detecting the structural differences among clay mineral groups in unfired samples. In XRD analysis, a powdered sample is exposed to a monochromatic beam of X-rays. When the beam hits a mineral's crystal lattice, the X-rays constructively and destructively interfere or diffract. The angles at which the X-rays diffract vary with the distance (d-spacing) between adjacent planes of atoms in the crystal, resulting in a distinctive diffraction pattern for every crystalline mineral. The measured angles of diffraction can be used to calculate the d-spacing (d) according to Bragg's law:

$$n\lambda = 2d\sin\theta \quad (1)$$

where n is an integer representing the order of the diffracted beam, λ is the wavelength of the incident beam, and θ is the angle between the diffracted beam and the crystallographic plane. Once the d-spacing is known, the mineral can be identified through comparison with standard reference materials (Flohr 1997; Stanjek and Häusler 2004).

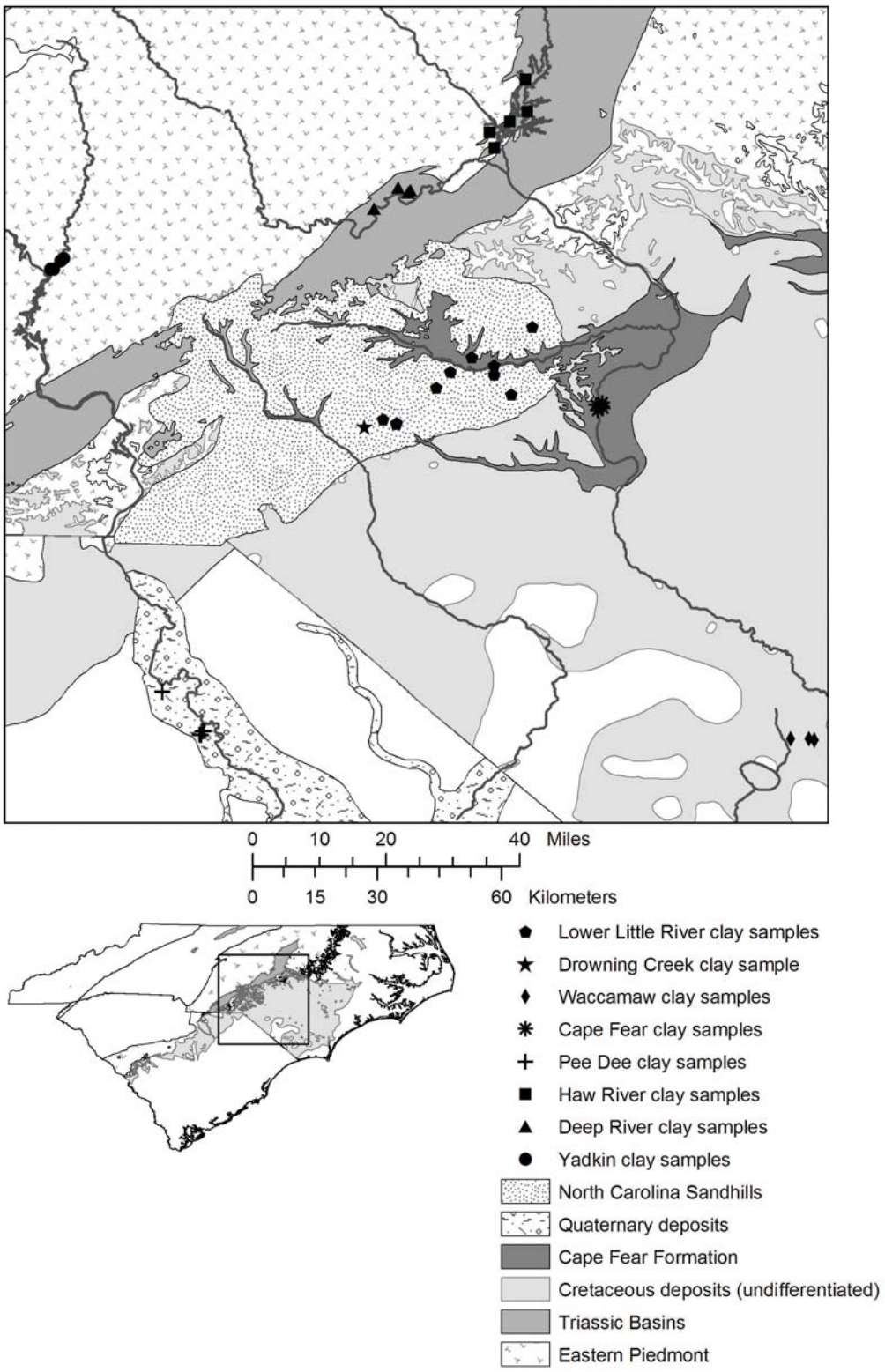

Figure 7.1. Locations of 42 clay samples analyzed by XRD (North Carolina Geological Survey 1998; South Carolina Geological Survey 2005; United States Geological Survey 2002).

Although standard XRD does not provide quantitative compositional data, several semi-quantitative methods can be applied to determine the relative proportions of minerals in a sample (Hurst et al. 1997). One such method, the Mineral Intensity Factor 100% approach (MIF), uses integrated diffraction peak intensities and reference intensity ratios to roughly estimate the *comparative* weight fraction of each mineral, assuming that the identified minerals constitute 100% of the sample (see Kahle et al. 2002 for a detailed description of this method). Although MIF has been criticized when represented as a quantitative technique (Kahle et al. 2002), it is an acceptable method of achieving semi-quantitative results for the purpose of comparing a similar suite of samples within a single study.

Methodology

Samples were air-dried and ground in a ball mill. Clay-sized particles (i.e., equivalent spherical diameter of 2 μm or less) were separated by allowing the larger fraction to settle in a column of water. In some cases, calcium phosphate chemicals were added to reduce flocculation and allow the particles to remain dispersed. The clay-sized fraction was then coated onto glass slides for preferred orientation and ethylene-glycol saturated analyses.

The specimens were analyzed on a Scintag XDS-2000 diffractometer using CoK_{α} radiation. Randomly-oriented (bulk) samples were run at a continuous scan rate of 1.00 degree per minute over a range of 2.00–70.00 degrees; counts were collected for 0.600 seconds at step increments of 0.010 degrees. Preferred orientation and ethylene-glycol saturated specimens were scanned at a continuous rate of 0.50 degrees per minute over a range of 2.00–36.00 degrees, with counts collected for 1.2 seconds.

Diffraction patterns for all three specimens (i.e., bulk, air-dried preferred orientation, and ethylene glycolated) were combined to qualitatively assess the abundance of ten minerals or mineral groups in each sample: quartz, lepidocrocite, gibbsite, plagioclase, K-feldspar, amphibole, the 7Å kaolin group, the 10Å illite/mica group, the 14Å hydroxy-interlayered vermiculite/chlorite/smectite group, and expandable (smectitic) clays.

The MIF procedure was applied to the bulk data to obtain semi-quantitative measurements of quartz, lepidocrocite, gibbsite, plagioclase, K-feldspar, amphibole, and total clay minerals. It was also applied to the preferred orientation data to assess the percentages of the 14Å, 10Å, and 7Å clay minerals relative to each other. Finally, the preferred orientation estimates were applied to the total clay mineral measurement from the bulk data to calculate semi-quantitative measurements for each of the three clay mineral groups.

Results

Qualitative analysis of bulk mineralogy suggests that clays from the same drainage basin generally exhibit similar mineral compositions (Table 7.1). Individual drainages cannot be differentiated on the basis of bulk mineral composition, but feldspar (i.e., plagioclase and K-feldspar) mineralogy does help discriminate between regions. With a few exceptions, clays from drainages originating in the Piedmont contain plagioclase and/or K-feldspar while those from drainages restricted to the Coastal Plain do not.

Table 7.2 presents the results of semi-quantitative analysis for 39 samples. All values represent the estimated proportions of minerals relative to each other and should not be confused

Table 7.1. Qualitative bulk mineralogy.[a]

Region/Drainage: Sample ID	Quartz	Lepidocrocite	Gibbsite	Plagioclase	K-feldspar	Amphibole	Clay Minerals: 14Å Group	10Å Illite/Mica	7Å Kaolin Group	Expandable (Smectitic)
Sandhills/Lower Little:										
FBR002	xx		x				x	x	x	
FBR003	xx		x				x	x	x	
FBR004	xx			x				x	x	x
FBR005	xx		tr	x			x	x	x	
FBR007	xx		x				x	x	x	tr
FBR008	xx						tr	x	x	
FBR009	xx							x	x	
FBR010	xx			x			x	x	x	tr
FBR017	xx	x					x	x	x	x
FBR059	xx						x	x	xx	
FBR067	xx						x	x	xx	
Sandhills/Drowning Cr:										
FBR006	xx						x	x	xx	
Coastal Plain/Waccamaw:										
FBR081	xx	x					x		x	tr
FBR082	xx						x	x	x	x
FBR083	xx						x		x	
FBR084	xx						x		x	x
FBR085	xx				tr		x		x	x
Coastal Plain/Cape Fear:										
FBR011	xx			x	x		x	x	x	tr
FBR012	xx			x	x		x	x	x	x
FBR013	xx			x	x		x	x	x	tr
FBR014	xx			x	x		x	x	x	x
FBR016	xx			tr	tr		x	x	x	x
Coastal Plain/Pee Dee:										
FBR019	xx	x	x	x	x		x	tr	x	
FBR020	xx		tr	x	x		x	x	x	
FBR021	xx		tr	x	x		x	x	x	
FBR023	xx			tr	tr		x	x	x	tr

Table 7.1. Qualitative bulk mineralogy (continued).[a]

Region/Drainage: Sample ID	Quartz	Lepidocrocite	Gibbsite	Plagioclase	K-feldspar	Amphibole	Clay Minerals: 14Å Group	10Å Illite/Mica	7Å Kaolin Group	Expandable (Smectitic)
FBR027	xx			tr	tr		x	x	x	
Piedmont/Haw:										
FBR029	xx			tr			x		x	x
FBR030	xx			tr			x	xx	x	
FBR035	xx			x	x		x	xx		x
FBR040	xx				x		x	tr		
FBR041	xx			x	x		x			x
Piedmont/Deep:										
FBR058	xx			x	tr	tr	x	x	x	tr
FBR071	xx			x			x	x	x	x
FBR074	xx			x			x	x	x	x
FBR077	xx			x			x	x	x	tr
FBR080	xx			x	tr		x	x	x	
Piedmont/Yadkin:										
FBR048	xx			x	tr		x	x	x	
FBR049	xx			x			x	x	x	
FBR051	xx			x		tr	x	x	x	
FBR054	xx			x		tr	x	x	x	
FBR055	xx			x		tr	x	x	x	

[a] Key: xx, abundant; x, minor; tr, trace.

Table 7.2. Semi-quantitative mineralogy.[a]

	Nonclay Minerals[b]						Clay Minerals[c]		
Region/Drainage: Sample ID	Quartz (%)	Lepidocrocite (%)	Gibbsite (%)	Plagioclase (%)	K-feldspar (%)	Amphibole (%)	14Å Group (%)	10Å Illite/Mica (%)	7Å Kaolin Group (%)
Sandhills/Lower Little:									
FBR002	84.9	0.0	3.6	0.0	0.0	0.0	4.3	4.3	2.8
FBR003	87.5	0.0	3.3	0.0	0.0	0.0	2.0	3.0	4.1
FBR004	88.2	0.0	0.0	1.2	0.0	0.0	8.9	0.4	1.2
FBR005	90.8	0.0	1.0	2.2	0.0	0.0	3.1	0.0	3.0
FBR007	82.8	0.0	1.2	0.0	0.0	0.0	1.4	8.4	6.2
FBR008	94.4	0.0	0.0	0.0	0.0	0.0	0.0	3.2	2.5
FBR009	86.3	0.0	0.0	0.0	0.0	0.0	0.0	8.2	5.5
FBR010	94.0	0.0	0.0	3.1	0.0	0.0	0.8	0.3	1.7
FBR017	77.1	12.6	0.0	0.0	0.0	0.0	9.3	0.0	1.0
FBR059	94.7	0.0	0.0	0.0	0.0	0.0	4.6	0.0	0.7
FBR067	49.8	0.0	0.0	0.0	0.0	0.0	14.3	0.8	35.0
Sandhills/Drowning Cr:									
FBR006	63.9	0.0	0.0	0.0	0.0	0.0	1.4	8.4	26.3
Coastal Plain/Waccamaw:									
FBR081	93.1	5.3	0.0	0.0	0.0	0.0	1.2	0.0	0.5
FBR082	96.5	0.0	0.0	0.0	0.0	0.0	3.1	0.0	0.4
FBR084	87.2	0.0	0.0	0.0	0.0	0.0	11.1	0.7	0.9
FBR085	82.5	0.0	0.0	0.0	0.6	0.0	13.5	2.5	0.9
Coastal Plain/Cape Fear:									
FBR011	70.1	0.0	0.0	7.2	16.0	0.0	4.8	0.0	1.9
FBR012	90.9	0.0	0.0	1.8	4.6	0.0	2.3	0.0	0.4
FBR013	89.8	0.0	0.0	2.2	2.4	0.0	3.4	1.2	1.0
FBR016	89.3	0.0	0.0	0.8	3.9	0.0	4.2	0.4	1.4
Coastal Plain/Pee Dee:									
FBR019	72.1	2.3	10.5	1.8	6.0	0.0	4.2	0.7	2.3
FBR020	69.3	0.0	14.5	1.8	3.9	0.0	6.2	1.0	3.3
FBR021	70.3	0.0	9.6	1.2	4.9	0.0	10.2	0.0	3.9

Table 7.2. Semi-quantitative mineralogy (continued).[a]

	Nonclay Minerals[b]						Clay Minerals[c]		
Region/Drainage: Sample ID	Quartz (%)	Lepidocrocite (%)	Gibbsite (%)	Plagioclase (%)	K-feldspar (%)	Amphibole (%)	14Å Group (%)	10Å Illite/Mica (%)	7Å Kaolin Group (%)
FBR023	84.4	0.0	0.0	0.3	1.7	0.0	4.2	2.5	6.9
FBR027	74.6	0.0	0.0	1.3	2.5	0.0	13.9	1.9	5.8
Piedmont/Haw:									
FBR029	97.2	0.0	0.0	0.5	0.0	0.0	0.6	1.2	0.5
FBR030	88.3	0.0	0.0	1.2	0.0	0.0	9.7	0.0	0.8
FBR035	88.2	0.0	0.0	0.9	4.1	0.0	2.4	3.6	0.8
FBR040	91.2	0.0	0.0	0.0	2.5	0.0	3.9	2.1	0.3
FBR041	87.9	0.0	0.0	0.9	2.3	0.0	6.8	1.9	0.3
Piedmont/Deep:									
FBR058	90.6	0.0	0.0	2.4	0.0	0.0	4.3	0.8	2.0
FBR071	88.1	0.0	0.0	5.1	0.0	0.0	1.9	0.0	4.8
FBR074	82.5	0.0	0.0	9.3	0.0	0.0	4.3	3.1	0.7
FBR077	90.1	0.0	0.0	4.8	0.0	0.0	4.7	0.3	0.0
FBR080	95.6	0.0	0.0	2.7	1.3	0.0	0.2	0.2	0.0
Piedmont/Yadkin:									
FBR048	90.1	0.0	0.0	4.4	0.0	0.0	4.8	0.5	0.2
FBR051	89.7	0.0	0.0	4.2	0.0	0.4	3.1	1.1	1.5
FBR054	92.8	0.0	0.0	3.4	0.6	0.3	1.9	0.0	1.1
FBR055	91.5	0.0	0.0	2.7	0.0	0.0	3.9	0.0	1.9

[a] All values represent the estimated proportions of minerals relative to each other.
[b] Based on bulk data.
[c] Based on bulk and preferred orientation data.

with absolute concentrations. Samples FBR014, FBR049, and FBR083 (from the Cape Fear, Yadkin, and Waccamaw drainages, respectively) have been omitted because of concerns regarding artifacts attributed to effects of preferred orientation on the diffraction patterns.

To facilitate identification of patterning in the semi-quantitative data, relative proportions of minerals were plotted on ternary diagrams in various combinations. Displaying the data this way reveals some general patterns with respect to feldspar and clay mineralogy.

Feldspar Mineralogy

It is not possible to demonstrate clear distinctions among individual drainages on the basis of semi-quantitative data for only 39 samples, but some differentiation is evident on the basis of feldspar mineralogy (Figure 7.2). Samples from the Haw drainage do not exhibit any patterning in feldspar mineralogy and are consequently not considered in much of the following discussion. The lack of grouping in the Haw River data may reflect the heterogeneous nature of the collection sites: FBR029 is from the Slate Belt; FBR030 is from the Deep River Triassic Basin; and FBR035, FBR040, and FBR041 are from the shores of man-made Jordan Lake.

Piedmont samples contain high relative proportions of plagioclase compared to Coastal Plain samples (Figure 7.2). Samples from drainages restricted to the Coastal Plain generally lack feldspar minerals entirely, while Coastal Plain samples collected from drainages originating in the Piedmont exhibit mixed mineralogies with intermediate proportions of plagioclase and relatively high K-feldspar contents.

The patterning in Figure 7.2 makes sense given the geological characteristics of the Piedmont and Coastal Plain regions (Chapter 2). Plagioclase phenocrysts are common in metamorphic rocks of the Carolina Slate Belt (Stoddard 2006), so we would expect Piedmont sediments derived from these rocks to be plagioclase-rich. We would also expect alluvial sediments from Coastal Plain rivers with Piedmont origins to contain some redeposited plagioclase. The K-feldspar in the Cape Fear samples presumably comes from the Cretaceous Cape Fear Formation, which is characterized by K-feldspar-rich quartz sands (Figure 7.1; Sohl and Owens 1991:193). It is not clear why the Pee Dee samples collected from Quaternary deposits also contain high relative proportions of K-feldspar, although the Pee Dee River may pick up alkali sediments as it traverses Cretaceous deposits north of the collection area. Another possible explanation is that the K-feldspar was contributed by aeolian sediments, as has been demonstrated elsewhere in the southeastern U.S. (Schroeder et al. 1997).

Three Lower Little River samples (FBR004, FBR005, FBR010) exhibit high relative proportions of plagioclase and are therefore exceptions to the aforementioned patterns. These three anomalous samples were collected from the Cape Fear Formation, whereas all other Lower Little River samples were collected from the Middendorf Formation. The Cape Fear Formation generally contains more plagioclase than the Middendorf (Sohl and Owens 1991:193, 198), but it is puzzling that these three samples do not also contain the K-feldspar that characterizes the Cape Fear Formation. Again, the explanation may involve some sort of aeolian process.

Clay Mineralogy

The clay mineralogy data suggest additional trends (Figure 7.3). The 14Å hydroxy-interlayered vermiculite/chlorite/smectite minerals dominate the clay mineralogy of most samples, although many Sandhills specimens are relatively enriched in 7Å kaolin-group minerals. With the exception of the Sandhills samples, Coastal Plain clays tend to be very rich in

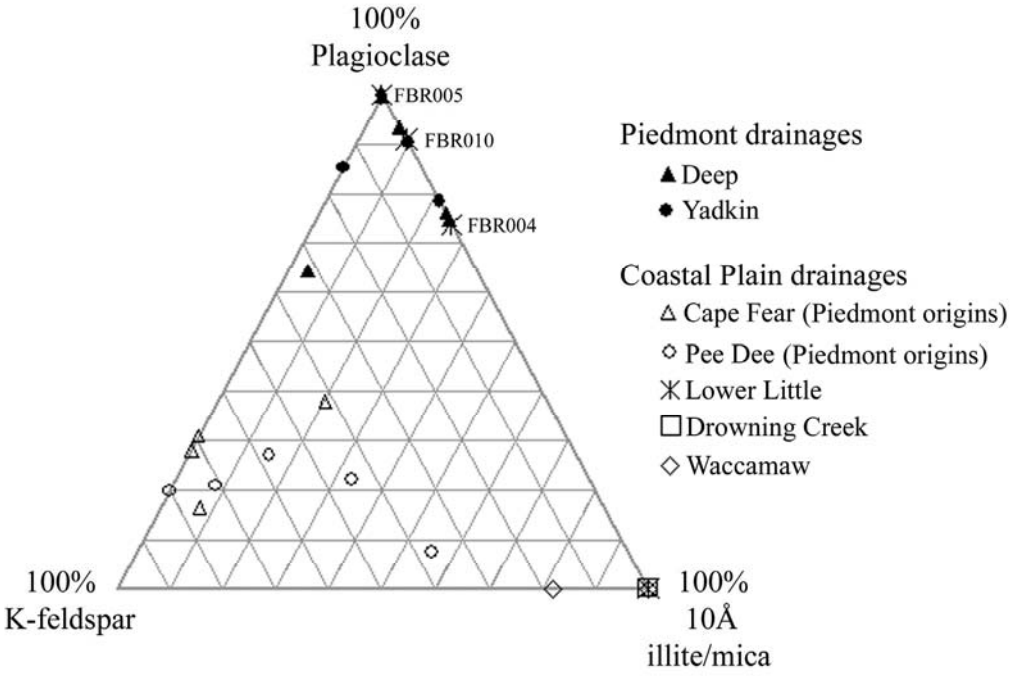

Figure 7.2. Clay samples plotted according to relative proportions of plagioclase, K-feldspar, and the 10Å illite/mica group minerals and arrayed by drainage. The labeled samples are discussed in the text. Samples from the Haw drainage do not exhibit any grouping in feldspar mineralogy and are not displayed.

14Å minerals and poor in 10Å illite/mica minerals. Piedmont clays, especially those from the Deep River Triassic basin, generally have low proportions of 7Å minerals.

The aforementioned patterns are consistent with the geology of the study area (Chapter 2). In general, Coastal Plain clays are rich in smectite-group minerals while Piedmont clays tend to be rich in kaolinite (Neiheisel and Weaver 1967; Steponaitis et al. 1996; Windom et al. 1971). It therefore makes sense that the Coastal Plain samples are relatively enriched in 14Å minerals, with those from Piedmont-spanning drainages exhibiting slightly higher proportions of 7Å minerals than those from the Waccamaw drainage. Most of the Sandhills samples that seem to be exceptions to the general rule come from the Middendorf Formation, which contains more kaolinite and illite than smectite in some areas (Heron 1960; Sohl and Owens 1991:196).

Piedmont clays that are rich in 14Å minerals and relatively deficient in kaolin-group minerals also seem to be exceptions to what we would expect to find. However, the 14Å mineral group includes hydroxy-interlayered vermiculite and chlorite, both of which are found in the Carolina Slate Belt. Furthermore, smectite-rich clays are common in the Deep River Triassic basin and in the vicinity of metagabbro intrusions, which are abundant in the area where the Yadkin samples were collected (Buol 2003; Olive et al. 1989; Schroeder and West 2005).

Discussion

A principal objective of the XRD analyses was to determine if mineralogical variability could account for the geochemical patterns identified in Chapter 5. An additional objective was

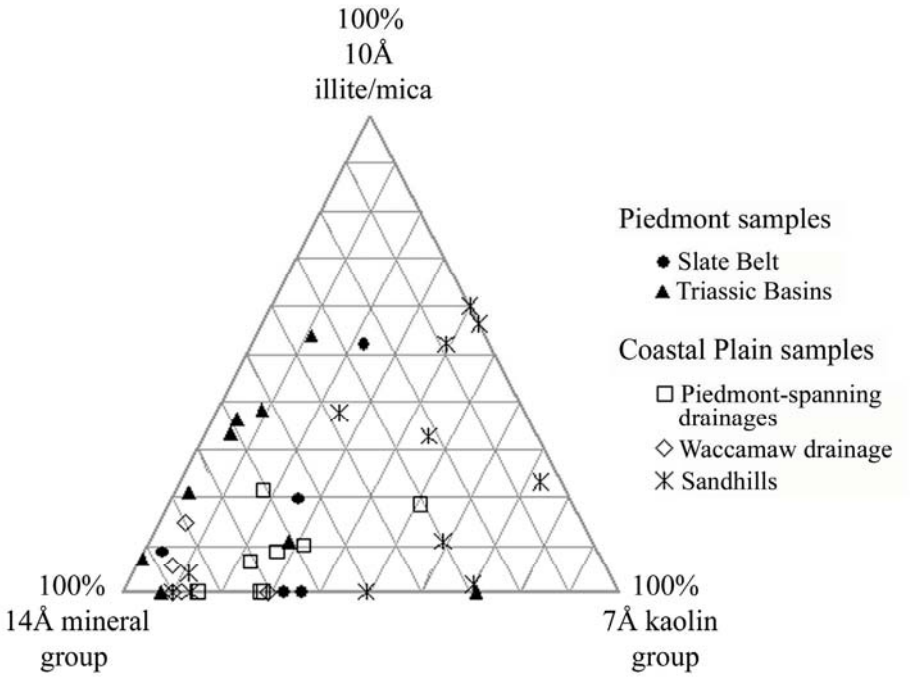

Figure 7.3. Clay samples plotted according to relative proportions of 10Å, 14Å, and 7Å minerals and arrayed by physiographic region.

to ascertain the extent to which clay mineralogy influences workability and other physical properties (see Chapter 4) that presumably formed the basis upon which prehistoric potters selected their clay resources.

Geochemistry

Neutron activation analysis data indicate that clay samples from Piedmont drainages (Deep, Yadkin) or Coastal Plain drainages originating in the Piedmont (Cape Fear, Pee Dee) have the greatest chemical similarity to Ca-rich Group 2 pottery (see Table 5.5, left side). Petrographic analyses (Chapter 6) suggest that the source of the Ca in these samples is plagioclase-rich igneous rocks from the Piedmont, and the results of the XRD analyses support this hypothesis. Our data confirm that clay samples from Piedmont-spanning drainages are generally enriched in plagioclase relative to samples from Coastal Plain drainages (Figure 7.2, Table 7.1).

Physical Properties

Prehistoric potters selected clay resources on the basis of physical properties such as workability, shrinkage, and the hardness of ceramics made from them (Rice 1987:53). Identifying the relationship between these physical properties and mineralogy could therefore help us understand why potters selected resources from particular areas. It could also help us predict additional locations where suitable resources are likely to be found. Mineralogical trends in the performance data consequently merit consideration.

Workability. Smectitic clays are generally more plastic than kaolinite-rich clays (Rice 1987:60), and indeed our good and moderately lean samples typically contain higher proportions of 14Å minerals than our lean samples (Figure 7.4). As explained in Chapter 4, however, our sample of lean clays does not represent the entire study area: lean materials were collected in the Sandhills region only. Furthermore, lean clays make up the majority of that region's samples. Thus the apparent mineralogical distinction between lean and more workable samples may simply reflect mineralogical differences between the Sandhills and other regions. The fact that the clay mineralogy data do not help discriminate between moderately lean and good samples supports the idea that the pattern in Figure 7.4 may be spurious. Nonetheless, it is interesting to note that the most workable sample from the Sandhills is also the richest in 14Å clay minerals (FBR017).

Better separation between moderately lean and good samples is achieved when feldspar mineralogy is considered (Figure 7.5). In general, good clays contain proportionally more K-feldspar and less plagioclase than moderately lean clays. Even the Haw River samples, which demonstrate no regional patterning with respect to feldspar mineralogy, fit this general pattern. Three good Haw River samples (FBR035, FBR040, and FBR041) are K-feldspar-rich and plagioclase-poor, while two moderately lean samples (FBR029 and FBR030) are plagioclase-rich and lack K-feldspar. Before a definite relationship between feldspar mineralogy and workability of Carolina clays can be posited, however, additional samples, including representative lean ones, should be analyzed to discredit the possibility that the pattern in Figure 7.5 is fortuitous.

Hardness. The relationship between feldspar mineralogy and ceramic hardness resembles the relationship between feldspar and workability: hard samples tend to contain proportionally more K-feldspar and less plagioclase than soft samples (Figure 7.6). This is not surprising given that most clay samples with good workability also yielded hard test tiles (see Chapter 4). K-feldspar can act as a flux, and modern potters often add it to their clays to lower the temperature at which sintering begins, increase fired strength, and reduce porosity (Rice 1987:75). It is possible that K-feldspar had a similar effect on some of our samples, especially those that were fired at 950ºC and show evidence of vitrification.

Drying Shrinkage. Kaolinite- and illite-rich clays typically shrink less during drying than smectitic clays (Goffer 1980:Table 8.3; Rice 1987:Table 2.7), and this observation holds true for many of our samples (Figure 7.7). Clays exhibiting high shrinkage values also tend to contain low proportions of plagioclase (Figure 7.8). Plagioclase occurs in many of our samples as relatively coarse inclusions and thus presumably reduces shrinkage by increasing pore space.

Conclusions

The XRD data help explain the geochemical patterning discussed by Speakman, Glascock, and Steponaitis in Chapter 5. They also suggest that K-feldspar and 14Å clay minerals may have a positive effect on workability. If this conclusion is valid, additional workable samples are likely to be found in areas characterized by these minerals. In particular, suitable raw materials may have been available just east of the Sandhills in the K-feldspar-rich Cape Fear Formation. We therefore recommend that future efforts to find suitable clays near the Sandhills should focus on the portion of the Lower Little drainage that cuts through the Cape Fear Formation.

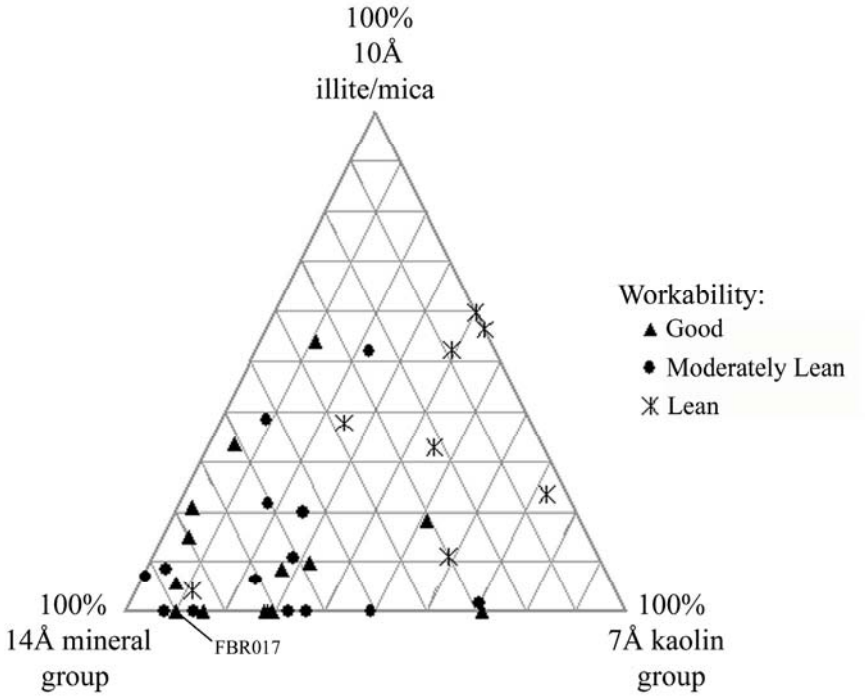

Figure 7.4. Clay samples plotted according to relative proportions of 10Å, 14Å, and 7Å minerals and arrayed by workability. The labeled sample is discussed in the text.

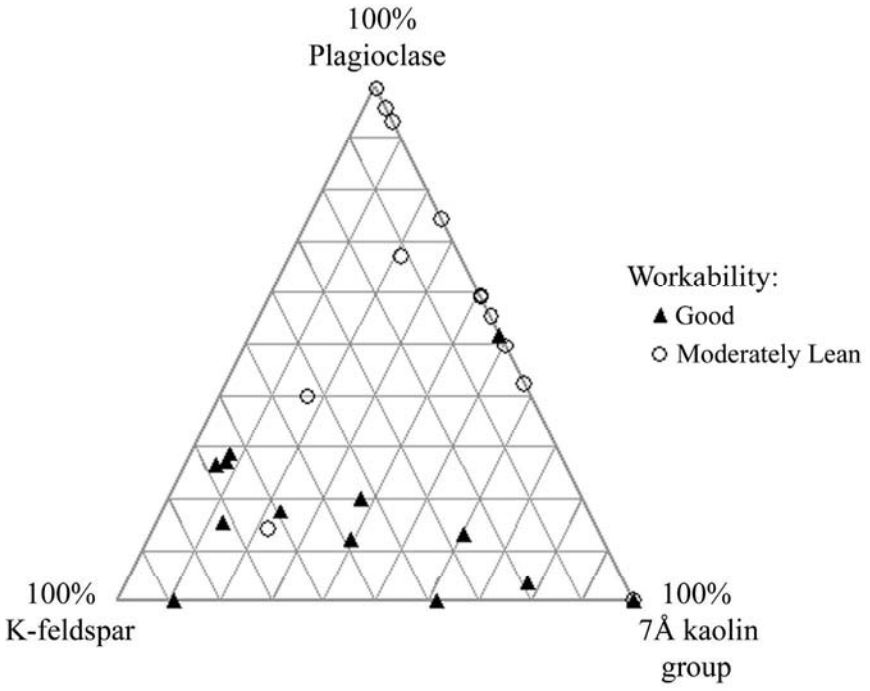

Figure 7.5. Good and moderately lean clay samples plotted according to relative proportions of plagioclase, K-feldspar, and 7Å minerals.

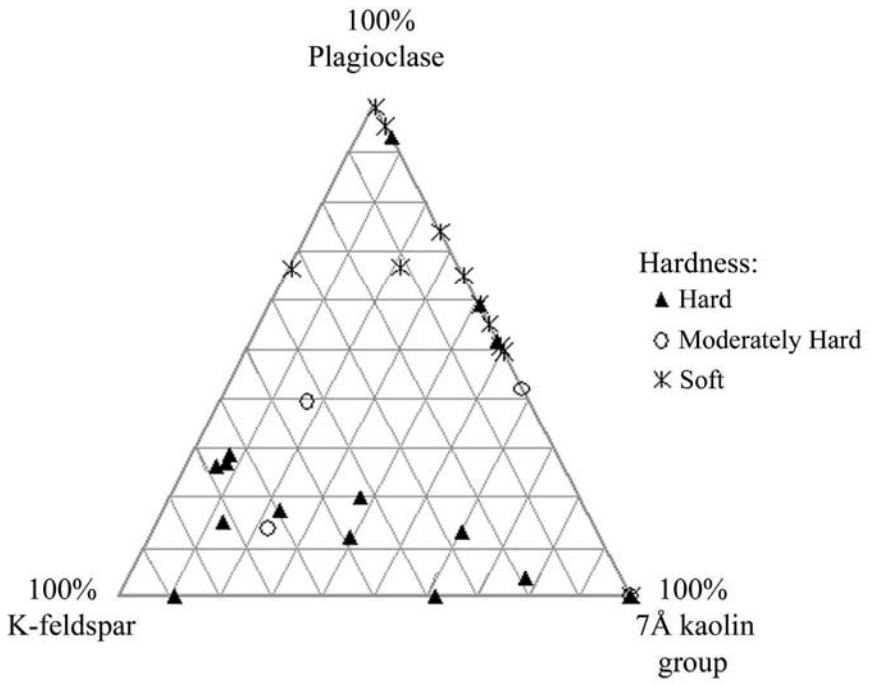

Figure 7.6. Clay samples plotted according to relative proportions of plagioclase, K-feldspar, and 7Å minerals and arrayed according to hardness.

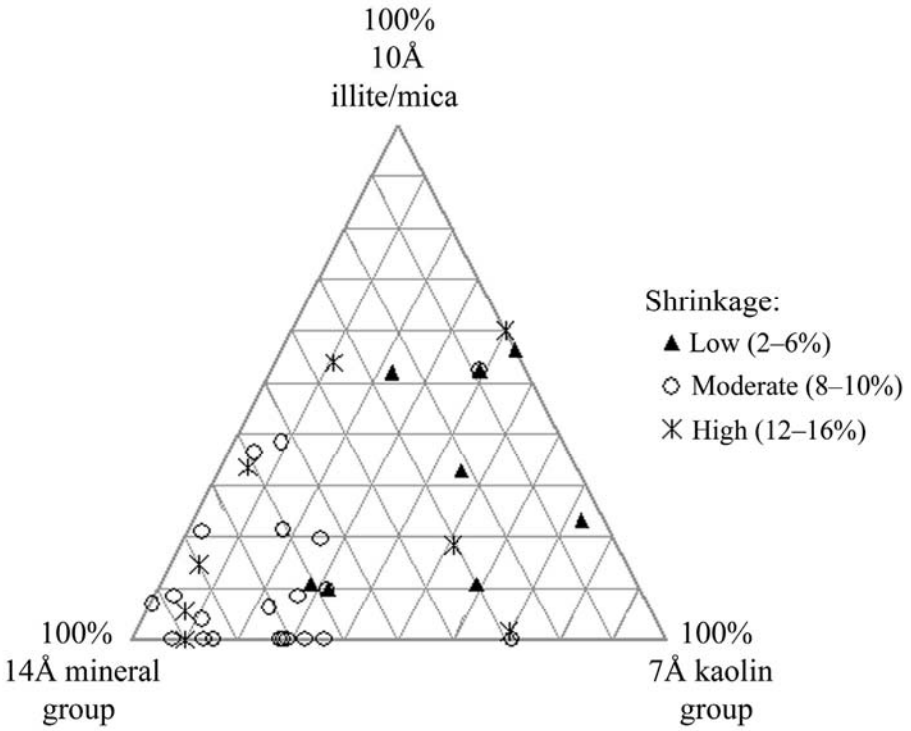

Figure 7.7. Clay samples plotted according to relative proportions of 10Å, 14Å, and 7Å minerals and arrayed according to linear drying shrinkage.

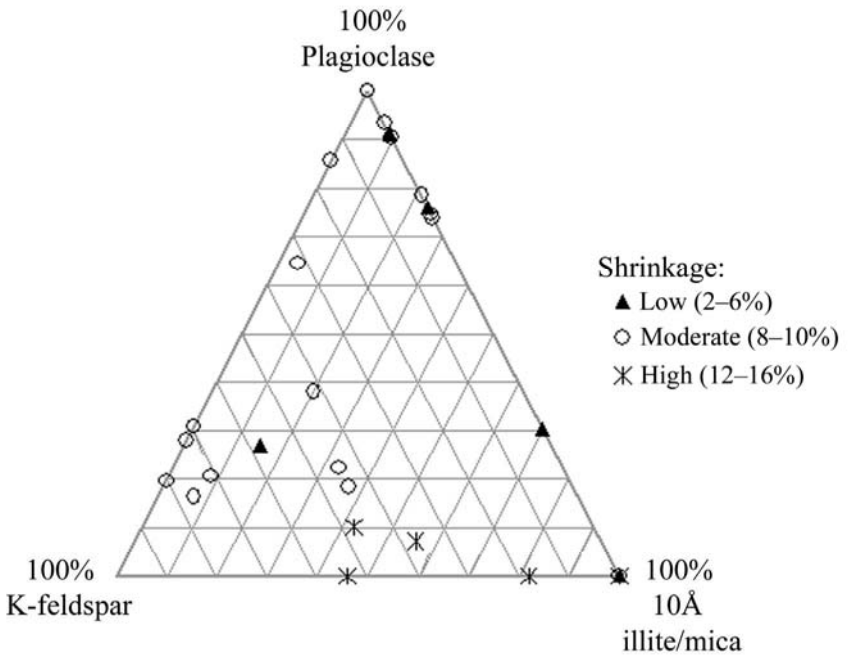

Figure 7.8. Clay samples plotted according to relative proportions of plagioclase, K-feldspar, and 10Å minerals and arrayed according to linear drying shrinkage.

Notes

Acknowledgments. We thank Charles W. Rovey for advice on applying the MIF procedure to the preferred-orientation data.